Desalination and Water Treatment
www.deswater.com
doi: 10.1080/19443994.2014.985725

57 (2016) 3572–3587
February

Taylor & Francis
Taylor & Francis Group

Biosorption of heavy metals from actual electroplating wastewater using encapsulated *Moringa oleifera* beads in fixed bed column

Kannan Radhakrishnan[a], Lakshmi Sethuraman[a], Radha Panjanathan[a], Aparna Natarajan[a], Vishali Solaiappan[b], Wilson Richard Thilagaraj[a,*]

[a]*Department of Biotechnology, School of Bioengineering, SRM University, Kattankulathur 603 203, Tamil Nadu, India, Tel. +91 8939944299; email: kannas2k@gmail.com (K. Radhakrishnan), Tel. +91 9489307608; email: laksbiotech@gmail.com (L. Sethuraman), Tel. +91 9443599966; email: radha.p@ktr.srmuniv.ac.in (R. Panjanathan), Tel. +91 9444888146; email: anusindu@yahoo.com (A. Natarajan), Tel. +91 9840712683; email: thilagaraj.richard@gmail.com (W.R. Thilagaraj)*
[b]*Department of Chemical Engineering, School of Bioengineering, SRM University, Kattankulathur 603 203, Tamil Nadu, India, Tel. +91 9443883562; email: meet.vishali@gmail.com*

Received 27 March 2014; Accepted 31 October 2014

ABSTRACT

In this study, encapsulated *Moringa oleifera* bead (EMB) was synthesized using *M. oleifera* seed powder with Ca-alginate for the biosorption of heavy metals (Zn^{2+}, Cu^{2+}, Mn^{2+}, Co^{2+}, and Ni^{2+}) from electroplating industrial wastewater. In batch mode, the effects of various experimental parameters (contact time, biosorbent mass, and pH) were investigated. Equilibrium modeling studies (Langmuir, Freundlich, Temkin, and Dubinin–Radushkevich) were established and the maximum sorption capacity (q_{max}) of about 5.8, 4.78, 4.6, 1.3, and 1.02 mg/g was reported for Co^{2+}, Ni^{2+}, Cu^{2+}, Zn^{2+}, and Mn^{2+}, respectively. Further, biosorption of heavy metals was carried out by fixed bed column studies by varying the parameters such as effect of influent flow rate (1–10 mL/min) and bed height (5–25 cm). Based on the experimental results, the breakthrough capacity ($Q_{0.5}$ mg/g) was acquired at 55.5, 63.1, 74.5, 64.9, and 104.5 for Zn^{2+}, Cu^{2+}, Mn^{2+}, Co^{2+}, and Ni^{2+} with influent flow rate of 1 mL/min. In addition, Thomas and Yoon–Nelson models were applied to the experimental data to predict the breakthrough curves using linear equation and to establish the distinctive parameters of the column. Finally, EMB was examined before and after biosorption using SEM/FTIR analytical techniques. In conclusion, based on our results, EMB is expected to be a competent biosorbent for the removal of heavy metals from the wastewater.

Keywords: Electroplating wastewater; Column study; Breakthrough curve; Heavy metals; *Moringa oleifera*; Biosorption

1. Introduction

Industrial wastewater plays a deteriorating role to the environment through the discharge of heavy metals from industrial wastewaters including the mining and metallurgy, electroplating industries, leather and ceramic industry, agro-chemical industries, etc. [1]. Heavy metals are recognized as the long-term hazardous contaminants to the environment due to their high toxicity, retention in the soil, and accumulation in the body. Based on their toxicity, Bureau of Indian

*Corresponding author.

Standards (IS:10500) has set the maximum permissible limit for heavy metals in drinking water (IS:10500) as follows: Zn^{2+}, 5 mg/L; Cu^{2+}, 0.05 mg/L; Mn^{2+}, 0.1 mg/L; Co^{2+}, 1 mg/L; and Ni^{2+}, 0.1 mg/L [2].

The harmful effects of heavy metals to human health in the environment are a challenge to ecosystem as well as human health. Ingestion of zinc and its compounds can result in a variety of chronic effects in the gastrointestinal, haematological, and respiratory systems along with alterations in the cardiovascular and neurological systems of humans. Excess intake of copper causes chronic severe cholestatic liver disease, irritation of mucosal and central nervous system, and hepatic and renal damage [3–6]. Exposure to manganese is inevitable, as it is widespread in the natural environment, and Mn^{2+} toxicity causes metal fume fever, pneumonitis, and pulmonary edema in liver [7,8]. Cobalt poisoning in human causes many chronic lung problems [9]. Severe exposure to nickel compounds causes rhinitis, sinusitis, anosmia, and in extreme cases leads to perforation of the nasal septum [10,11]. The International Agency for Research on Cancer classified nickel compounds as carcinogenic to human.

Based on previous reports, it is noted that many of the treatment technologies suggested for the removal of heavy metals include chemical precipitation, ion-exchange, coagulation [12], adsorption [13], and some biological methods. However, most of these methods require high operational cost and energy requirement. Among these technologies, adsorption is the only method to handle large volume of wastewater in batch as well as fixed bed column operation, and it is the simplest and efficient method to remove the trace amount metal ions from the effluent. In recent studies, a variety of natural sorbents such as natural clinoptilolite [14], natural cotton fibre [15], eggshell membrane [16], and tamarind fruit shell [17] has been reported for the removal of heavy metals under batch operation. Many of these sorbents have low-sorption capacity and slow kinetics, and explicitly used for single metals. Moreover, several studies have confirmed fixed bed column as the most efficient for cyclic sorption for the removal of heavy metals using granular activated carbon [18], calcined-star fish [19], chelating resin [20], and wheat straw [21] but these studies are restricted with smaller number of metals, and further research work is required.

Biosorption capacity of the sorbents obtained from batch equilibrium method provides fundamental information but this data is not applicable for real time process. In this connection, fixed bed column study is necessary to obtain process engineering data for scaling up from bench-scale to pilot-scale studies. Several studies have reported that plant based coagulants such as *Moringa oleifera* seeds [22], leaves [23], and bark [24] are used effectively for the removal of single metal ions, but there is not much study on using *M. oleifera* seed powder material using fixed bed column for treating industrial wastewater. Hence, this present work evaluated the performance of single biosorbent namely dried *M. oleifera* (MO) seed powder cross-linked with Ca-alginate, to obtain stable beads, and used for the treatment of electroplating wastewater that contains complex metals such as Cu^{2+}, Zn^{2+}, Co^{2+}, Mn^{2+}, and Ni^{2+}. The biosorbent was evaluated in batch mode for the removal of complex ions, and equilibrium studies were performed. Subsequently, the performance of the beads in a continuous column mode was investigated. In continuous mode, fixed bed column packed with encapsulation of *Moringa oleifera* bead (EMB) with respect to bed height and influent flow rate was studied for the removal of complex metal ions. Eventually, the breakthrough curve for the biosorption of heavy metals using Yoon–Nelson and Thomson models was analyzed.

2. Materials and methods

2.1. Adsorbate-electroplating effluent

The wastewater was collected from the settling tank during the secondary treatment process in the electroplating industry at Coimbatore, India. The characterization of electroplating wastewater was analyzed, according to the standard methods and trade effluent discharge standards by Central Pollution Control Board (CPCB) were tabulated in Table 1.

2.2. Biosorbent EMB

Dry *M. oleifera* seeds were purchased from Genius seeds, Coimbatore, India. The MO seeds were de-shelled and washed with de-ionized water, air-dried, and the pulverization process was carried out to get a fine powder, which was encapsulated by cross-link polymerization of sodium alginate and calcium chloride. In order to improve the properties of the beads, the powdered alginate was dissolved in a phosphate-buffered saline solution to form a viscous solution with different concentrations (varying from 1–3%) and the results were tabulated in Table 2. After mixing 1:5 ratios of the *M. oleifera* seed powder and viscous solution, they are allowed to fall drop wise in 3% (w/v) sterile calcium chloride solution with the help of a peristaltic pump. The flow rate of the pump was adjusted to be 250 spherical beads per hour. After encapsulation, the beads in the salt solution were

Table 1
Characterization of electroplating wastewater and CPCB-electroplating industrial discharge limit

Parameters	Initial electroplating wastewater	CPCB–Electroplating industrial discharge limit
pH @ 25°C	2.1	6.0–8.5
Conductivity (mS/cm)	6.9 ± 0.05	NA
Color (visual method)	Dark brown	Colorless
BOD (mg/L)	151	15
COD (mg/L)	486	40
TDS (mg/L)	14,896	2,100
Oil and grease (mg/L)	21	10
Zinc (mg/L)	24.15 ± 0.5	5
Copper (mg/L)	5.324 ± 0.15	3
Manganese (mg/L)	116.08 ± 0.5	5
Cobalt (mg/L)	9.088 ± 0.05	0.5
Nickel (mg/L)	6.704 ± 0.5	3
Cadmium (mg/L)	Trace amount	2
Chromium (mg/L)	Trace amount	2

Table 2
Characterization of encapsulated EMB

S. No.	Parameters	Values
1.	Porosity (%)	40–45
2.	Bulk density (g/cm^3)	1.5
3.	Stability	Stable and rigid
4.	Mean diameter (mm)	3.0 ± 0.1
5.	BET surface area (m^2/g)	14.5
6.	Q_{max} (cm^3/g)	0.0167
7.	Pore volume (cm^3/g)	0.05

incubated at room temperature for 2 h for the complete replacement of ions and then beads were stored at 4°C [25,26]. Before using the beads, the moisture content was removed by desiccators to prevent the damage of the pores.

2.3. Chemicals

All the chemicals used were of analytical grade .The chemicals like sodium alginate and calcium chloride were obtained as powdered form from HiMedia, Mumbai, India. The reagents, namely copper (II) chloride, zinc sulphate, and manganese chloride, were purchased from HiMedia, Mumbai and cobalt sulphate as well as nickel chloride were obtained from Ranbaxy, New Delhi. All the chemicals were used without further purification and the deionized water was prepared using purified water system (Milli G Dir 8).

2.4. Instrumental analysis

The surface morphology of EMB was examined by scanning electron microscope (SEM) using Agilent Technology (8500 FE-SEM). The functional groups of EMB were determined by Fourier Transform Infrared (FTIR) using an ALPHA FTIR spectrometer. Further, the amount of heavy metals concentration was analyzed by atomic absorption spectrometer (AAS) using AAS-4141.

2.5. Batch mode biosorption studies

Batch biosorption studies were carried out with 25 mL of the wastewater with known pH in a 250-mL Erlenmeyer flask and added EMB with different biosorbent mass from 2 to 10 g/L. The flask was in a quivering condition at an agitating speed of 150 rpm. After an equilibrium line, the biosorbent was separated and the metal concentration in the effluent was analyzed at regular time intervals, till the equilibrium concentration was reached. The influence of initial pH on metal biosorption was analyzed in the range of 2–10. One set of experiment was conducted using Ca-alginate beads, which is free from *M. oleifera* and it was noticed that there is no reduction of heavy metals. The amount of metal ions adsorbed onto the biosorbent was calculated by Eq. (1):

$$q_e = \frac{(C_o - C_e)V}{m} \quad (1)$$

where q_e (mg/g) is the amount of metals adsorbed at equilibrium, C_o and C_e are the initial and equilibrium

concentration of metals, respectively, V is the adsorbate volume (mL), and m is the mass of the biosorbent (g) [2]. Equilibrium modeling studies have been analyzed using different models such as Langmuir, Freundlich, Temkin, and Dubinin–Radushkevich (D–H) models.

2.6. Fixed bed biosorption studies

The schematic diagram of the fixed bed column in this study is shown in Fig. 1. The fixed bed column was made of Pyrex glass having the dimension of inner diameter of 4.5 cm and height of 55 cm. A sieve made up of stainless steel was placed at the bottom of the column. Over the sieve, a layer of glass wool was placed to prevent loss of biosorbent. The EMB was packed above the glass wool to the required bed height. A peristaltic pump (Model Masterfiex, Cole-Parmer Instrument Co., USA) was used to pump the feed stream (influent) through the column and the desired flow rate was controlled by the pump itself. A Rotameter was used to monitor the hydraulic loading rate, which is incorporated in the feed line of the column. The treated wastewater samples were collected at regular time intervals from the outlet of the column and the metal concentrations of effluent were periodically analyzed by AAS. All the biosorption experiments were carried out at the room temperature. Effect of bed height (Z: 5–25 cm) and inlet feed flow rate (Q_F: 1–10 mL/min) were investigated, and Thomas and Yoon–Nelson models have been formulated from the prediction of the breakthrough curve [18].

2.6.1. Theory-breakthrough analysis

For the determination of breakthrough curves, the fixed bed column was packed randomly with EMB and there is a continuous flow of the influent into the column until the wastewater concentration at the outlet stream becomes equivalent to the inlet stream. In a fixed bed column, the biosorbent located at the entry point of the influent, which is known as mass transfer zone (MTZ), comes in contact with the solution at its highest concentration level (C_o). As the time proceeds, this MTZ saturates rapidly and this zone starts moving downwards through the column of the next zone. When the biosorption zone reaches the exit of the bed, the concentration of the biosorbent in the effluent becomes equal to the influent concentration. The biosorption performance of the column is calculated by plotting the outlet concentration C_{out}/C_o as a function of time or volume throughout the curve known as breakthrough curve [27,28]. The time taken for the effluent concentration to reach a specific breakthrough concentration of interest is called breakthrough time (t_b). The breakthrough time for each of the column operation was defined as the time when the effluent concentration (C_t) reaches 50% of the initial

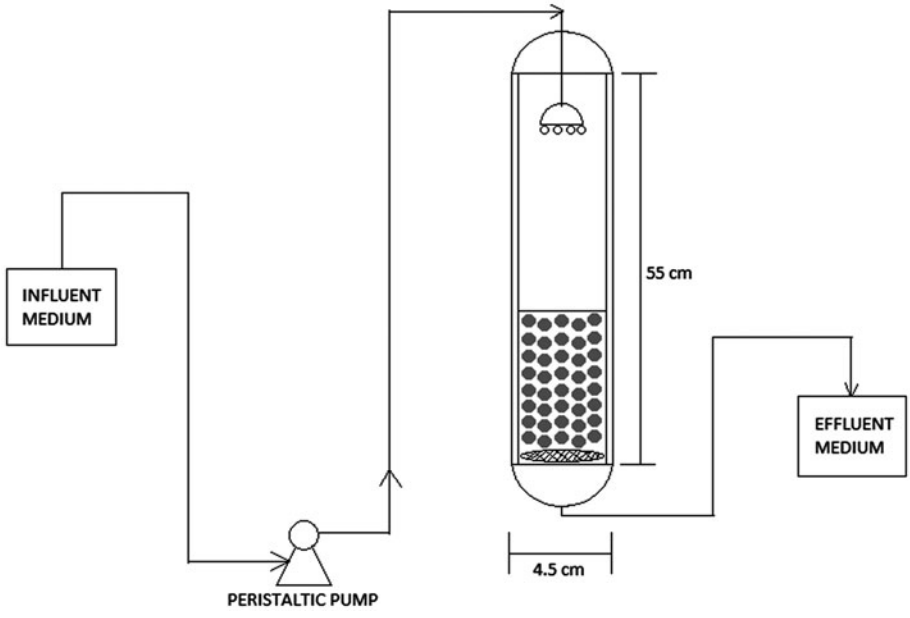

Fig. 1. Schematic diagram of continuous fixed bed column.

concentration (C_o). The capacity of the bed at breakthrough point is calculated from Eq. (2), which is given as:

$$q_b = \frac{C_o}{m}\int_0^{Vb}\left(1-\frac{C_t}{C_o}\right)dV \quad (2)$$

where q_b is the bed capacity at the breakthrough point (mg/g), C_o is the initial metal concentration (mg/L), m is the biosorbent mass, C_t is the exit metal concentration (mg/L), and V_b is the volume processed at breakthrough point [27].

Further, the numbers of bed volumes (BV) are established before the breakthrough point is reached to find the performance of the fixed bed adsorber which is directly related to the bed volume. Subsequently, bed exhaustion rate (BER) and empty bed resistance time (EBRT) were investigated to check the rate of exhaustion of beds. The BV is expressed as an Eq. (3):

$$\mathrm{BV} = \frac{\text{Volume of effluent treated at breakthrough point (L)}}{\text{Volume of adsorbent bed (L)}} \quad (3)$$

The BER and EBRT are expressed in the Eqs. (4) and (5):

$$\mathrm{BER} = \frac{\text{Mass of beds in packed bed column}}{\text{Volume of effluent treated at breakthrough point (L)}} \quad (4)$$

$$\mathrm{EBRT} = \frac{\text{Fixed bed volume}}{\text{Volume of flow rate of the effluent}} \quad (5)$$

The design of the column depends on the effect of operational parameters like inlet feed flow rate and various bed heights for the biosorption performance. The effects of these parameters on the removal of heavy metals (Zn^{2+}, Cu^{2+}, Mn^{2+}, Co^{2+}, and Ni^{2+}) using EMB were investigated.

2.7. Statistical analysis

Batch and column experiments were conducted in triplicates ($n = 3$) and all the data revealed are the mean values represented with the error bar. Correlation coefficients and standard deviations were calculated using SPSS PC+TM statistical package (1983). Multiple mean comparisons were computed using least significant difference (LSD) and significance level is $p < 0.05$.

3. Results and discussion

3.1. Characterization of the biosorbent

The FTIR spectra of EMB before and after biosorption were examined by triggering the molecular vibrations through irradiation with IR light which provided the information about the presence or absence of certain functional groups as shown in Fig. 2. From Fig. 2 (BB), spectrum shows the broadband peak centerd at 3,500–3,422 cm^{-1} which can be attributed to N–H stretching in the bondage of amides, and also associated to O–H stretching which is related to the presence of cationic and anionic amino acids. These amino acids might be contributed by the proteins present in the MO seeds which have also been reported in the previous study [29]. The band shown at 2,926 and 2,854 cm^{-1} corresponds to asymmetric and symmetric stretching at C–H of CH_2 groups, respectively. The combining features of amines and ketones which has both N–H band and the C=C band can be observed in the spectrum between 1,800 and 1,600 cm^{-1} representing amide functional group [30]. On the other hand, an FTIR spectrum of Fig. 2(AB) shows the disappearance of the broadband peak at 3,422 cm^{-1} and reduced intensity of peaks at 2,926 and 2,854 cm^{-1}, which is due to the mechanism of cross-linking of EMB which could be either by deprotonation or ionic interaction. Further, the SEM enables the direct observation of changes in the surface microstructures of the beads due to the modifications. Study of the SEM micrographs of EMB in Fig. 3(a) [EMB-BA] shows lot of cracks and also represents the presence of asymmetric pores and open pore structure, which provides high internal surface area on the surface of EMB, which is favorable for biosorption [1]. Subsequently, Fig. 3(b) [EMB-AA] indicates that after

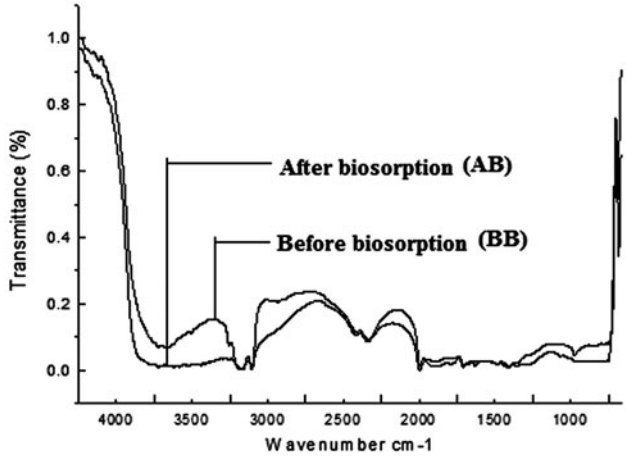

Fig. 2. (a) and (b) FTIR spectra of EMB before biosorption (BB) and after biosorption (AB).

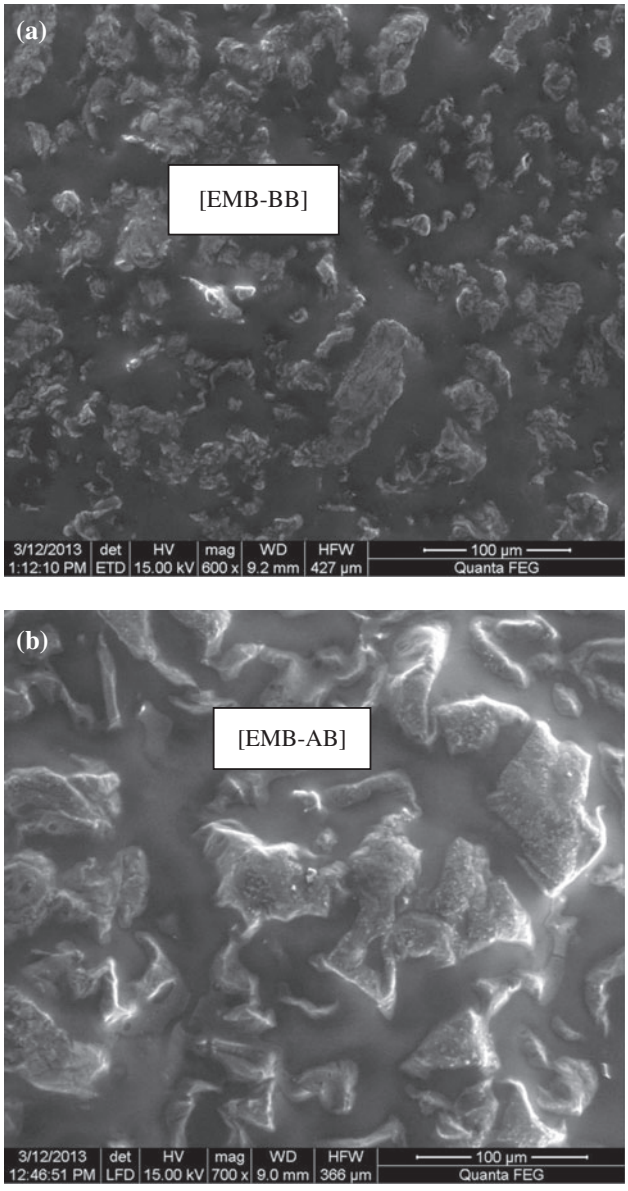

Fig. 3. (a) SEM image of before [EMB-BA] and (b) SEM image of after biosorption [EMB-AA].

biosorption there is clear demarcation in the surface morphology and pores were completely packed by the binding of heavy metals.

3.2. Batch mode biosorption study

3.2.1. Effect of initial pH and pH_{zpc} on biosorption

By changing the initial pH of the effluent, the uptake of the heavy metals was strongly affected on the surface charge of the biosorbent. As a result, the effect of pH on the biosorption of heavy metals onto EMB in the effluent was evaluated in the range of 2–10 with a contact time of 2 h at 303 K. The effect of pH on the biosorption can be explained on the basis of point of zero charge (pH_{zpc}), which is the point at which the net charge of the adsorbent is zero. The pH at pH_{zpc} of the EMB was determined by the solid addition method [31] and it was found to be 4.9–5.1, which in turn indicates that the surface is positively charged. The adsorption mechanism of heavy metals could be through the positive metal ions that form a bridge among the anionic polyelectrolyte and negatively charged protein functional groups on the particle surface [32]. From the experimental results, it is clearly seen that increase in the pH from 2 to 10 of the effluent appreciably caused for an apparent decrease in the biosorption of heavy metals as shown in Fig. 4. Quantitatively, it was observed that increasing the pH from 2 to 10 caused decrease in biosorption from 86.77 to 30% (Cu^{2+}), 77.20 to 30.5% (Ni^{2+}), 51.52 to 0.5% (Zn^{2+}), 49.77 to 45% (Mn^{2+}), and 43.85 to 20% (Co^{2+}), respectively. At $pH < pH_{zpc}$, positive surface sites are predominant, however some negative charge sites are also present in the surface. The maximum removal was observed at acidic pH 2 [i.e. actual pH of the wastewater is 2.1]. It is economical and convenient aspect to conduct the treatment at actual pH itself. The results were reliable with previous studies conducted by Fang et al. with electroplating effluents using sulfide from a sulfidogenic bioreactor effluent, achieved more than 90% at lower pH for complex metal ions (Cu^{2+}, Zn^{2+}, Ni^{2+}, and Fe^{2+}) [33]. Likewise, the results are consistent for the removal of Mn^{2+} using manganese oxide-coated carbon nanotubes by Taffarel and Rubio [34].

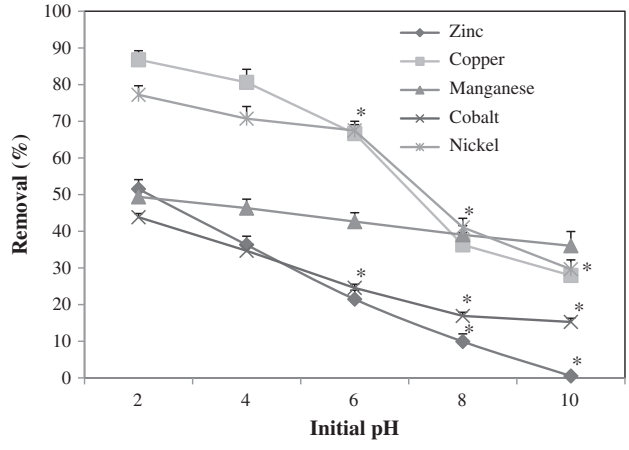

Fig. 4. Effect of initial pH on biosorption of heavy metal ions. [Conditions: effluent volume: 25 mL; initial pH 2–10; temperature: 303 K; contact time: 2 h; adsorbent mass: 5 g; agitation speed: 150 rpm; error bars represent SD.]

3.2.2. Effect of biosorbent mass

The effect of biosorption of metal ions onto EMB was studied by changing the quantity of biosorbent from 2 to 10 g/L in the effluent while maintaining other parameters as constant, (i.e. actual pH, 2.1 of the wastewater; agitation speed, 150 rpm; and temperature, 303 K) and the biosorption of metal ions at various masses is illustrated in Fig. 5. It can be seen that removal of heavy metal increases from 44 to 95.40% for Cu^{2+}, 27.68 to 79.98% for Ni^{2+}, 21 to 68.89% for Co^{2+}, 12.25 to 60.15% for Zn^{2+}, and 27.68 to 53.45% for Mn^{2+} from 2 to 10 g/L. In all the five metal cases, the amount of metal ions adsorbed increases with increase in biosorbent mass. This might be due to the fact that the number of active sites per gram of biosorbent increases proportionally and apparently, and the extent of sorption efficiency also increases [2,30]. When biosorbent ratio is small, the active sites for binding the metal ions on the biosorbent surface are less, so the biosorption efficiency is low. Similarly, when biosorption ratio is more, the efficiency is more [1]. Thus, it results in the increment of biosorption efficiency until saturation.

3.2.3. Effect of contact time

The removal of heavy metals as a function of contact time was investigated by varying the time from 0 to 130 min, while maintaining other parameters (biosorbent mass, 5 g; agitation speed, 150 rpm; and temperature, 303 K) as constant. The obtained results shown in Fig. 6 clearly reveals that there is a sharp uptake of metal ions in the beginning (0–60 min) and

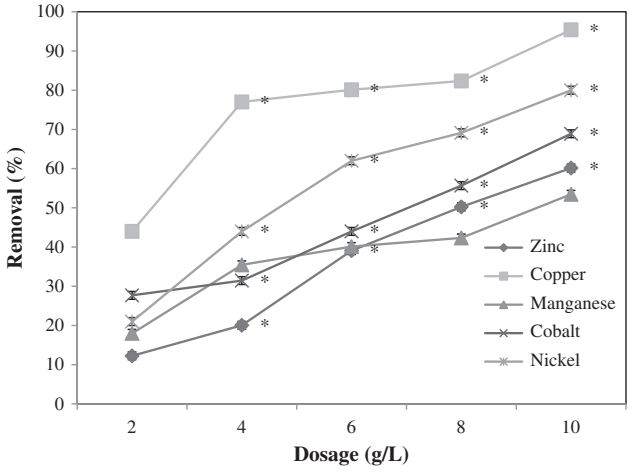

Fig. 5. Effect of biosorbent mass on biosorption of heavy metal ions. [Conditions: effluent volume: 25 mL; initial pH–actual pH of the effluent (2.1); temperature: 303 K; contact time: 2 h; adsorbent mass: 2–10 g/L; agitation speed: 150 rpm; error bars represent SD.]

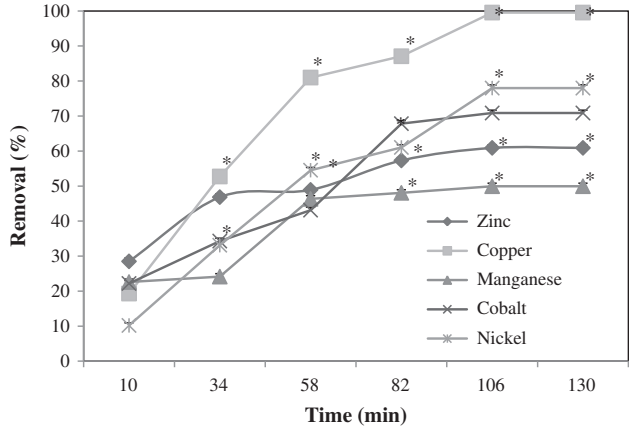

Fig. 6. Effect of contact time on biosorption of heavy metal ions. [Conditions: effluent volume: 25 mL; initial pH–actual pH of the effluent (2.1); temperature: 303 K; contact time: 0–130 min; adsorbent mass: 10 g/L; agitation speed: 150 rpm; error bars represent SD.]

gradually the biosorption slowed down at 60 to 100 min, and attained the equilibrium stage in the range of 100–130 min. At the initial contact time, there was a fast biosorption of metal ions due to the availability of the negatively charged surface on EMB, which leads to fast electrostatic attraction to metal ions. Once the biosorption of heavy metals on the external surface attains saturation and it takes longer time for the metal ions to diffuse and enter into the internal pores of the biosorbent particles to achieve equilibrium phase. Therefore, the rate of biosorption of metal ions onto EMB becomes time consuming and attained equilibrium stage at 130 min [35]. Fig. 6 indicates that the maximum percentage removal of metal ions as follows: Cu^{2+}, 99.54%; Ni^{2+}, 77.98%; Co^{2+}, 70.86%; Zn^{2+}, 60.90%; and Mn^{2+}, 49.96% at 130 min.

3.3. Biosorption isotherms

In order to examine the fundamental understanding behavior of the carrier matrix of biosorbent (EMB) and the practical design of the systems, the adsorption isotherm is essential and it is discussed by four well-known isotherm models including Langmuir, Freundlich, Temkin, and D–R models. Moreover, the maximum biosorption capacity, surface properties, and affinity of the biosorbent were investigated through the modeling of isotherms.

3.3.1. Langmuir model

The Langmuir model [36] assumes that metal biosorption occurs on a homogenous biosorbent surface

of active sites which are equally available and there is no transmigration of biosorbent in the plane of the surface. Based upon these assumptions, Langmuir represented the linear form of Eq. (6) as follows:

$$\frac{C_e}{q_e} = \frac{1}{q_{max} K_L} + \frac{C_e}{q_{max}} \quad (6)$$

where C_e is the equilibrium concentration (mg/L) of the metals in the effluents, q_e is the amount of metal adsorbed per gram of the biosorbent (mg/g) at equilibrium, q_{max} is the maximum monolayer coverage capacity (mg/g), and K_L is the Langmuir isotherm constant (L/mg) related to free energy of biosorption. The values of q_{max} and K_L were calculated from the slopes ($1/q_{max}$) and intercepts ($1/q_{max}K_L$) of the linear plots of C_e/q_e vs. C_e, respectively, (shown in Fig. 7) and the values are presented in Table 3. The linearity plots and the correlation coefficients (R^2) higher than 0.9 revealed that the EMB was well fitted and followed by Langmuir model. The maximum biosorption capacity (q_{max}) was found to be 5.8, 4.78, 4.6, 1.3, and 1.02 mg/g for Co^{2+}, Ni^{2+}, Cu^{2+}, Zn^{2+}, and Mn^{2+}, respectively, as shown in Table 3.

EMB biosorption was further analyzed in terms of separation factor R_L, which is a dimensional parameter defined as $R_L = (1/1 + K_L C_i)$, derived from the Langmuir equation and C_i is the initial metal concentration. R_L indicates the biosorption process to be either favorable ($0 < R_L < 1$), unfavorable ($R_L > 1$), linear ($R_L = 1$), or irreversible ($R_L = 0$). R_L values were in between 0 and 1, which indicates the process is more favorable Table 3.

3.3.2. Freundlich model

The Freundlich model [37] is an empirical equation based on sorption on heterogeneous surfaces through a multilayer adsorption mechanism which explains the reversible biosorption [32]. The logarithmic form of the Freundlich Eq. (7) can be expressed as follows:

$$\ln q_e = \ln K_{Fr} + \frac{1}{n} \ln C_e \quad (7)$$

where K_{Fr} ($mg^{1-1/n}\ L^{1/n}/g$) is the Freundlich constant which gives the relative biosorption capacity of the biosorbent, and $1/n$ is the dimensionless Freundlich biosorption intensity value. Values of K_{Fr} and $1/n$ can be determined by plotting ln q_e vs. ln C_e which results in a straight line with a slope of n and an intercept of ln K_{Fr}. Higher value of K_{Fr} estimates higher affinity toward the ions and the value of $1/n$ lies in-between

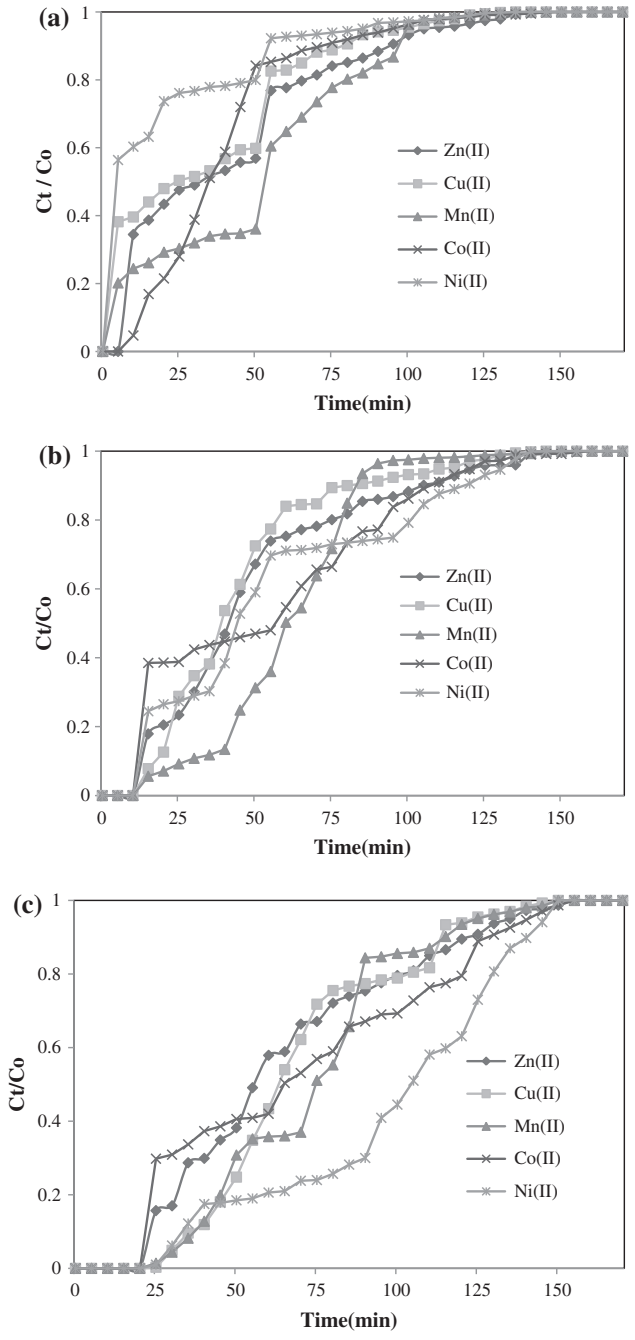

Fig. 7. ((a), (b), and (c)) Effect of bed height on biosorption of heavy metal ions in fixed bed column. [Conditions: Bed height: 5, 10, and 25 cm; influent flow rate: 1 mL/min; temperature: 303 K.]

$0.1 < 1/n < 1$ which represents the favorable biosorption. The correlation coefficients (R^2) values were higher than 0.9 (Table 3) indicating that the experimental data were also found to be fitting well with Freundlich isotherm model. The relative biosorption capacity was found to be 13.85, 8.988, 3.709, 2.632, and

Table 3
Equilibrium isotherm parameters for biosorption of heavy metals onto EMB

Heavy metals	Langmuir				Freundlich				Temkin				Dubinin–Radushkevich			
	q_{max} (mg/g)	K_L (L/mg)	R^2	ARE (%)	K_F ($mg^{1-1/n}1^{1/n}$/g)	n	R^2	ARE (%)	B (J/mol)	K_T (L/mg)	R^2	ARE (%)	q_{max} (mg/g)	E_S (kJ/mol)	R^2	ARE (%)
Zn	1.303	0.332	0.98	4.55	2.632	5.681	0.95	3.88	0.176	244.69	0.95	10.14	6.035	7.453	0.562	2.34
Cu	4.651	1.972	0.94	3.16	8.988	2.183	0.97	2.34	0.458	120.78	0.97	11.12	2.157	6.741	0.876	4.54
Mn	1.015	0.072	0.99	4.09	13.85	16.94	0.99	3.51	0.059	2.227	0.99	7.87	0.443	7.45	0.988	4.02
Co	5.882	0.148	0.95	8.76	1.190	9.433	0.93	7.89	0.106	5.160	0.93	7.65	4.399	5.454	0.951	3.34
Ni	4.784	2.348	0.91	3.24	3.709	3.389	0.94	3.29	0.295	84.77	0.94	2.34	2.134	7.453	0.932	5.55

1.190 mg/g for Mn^{2+}, Cu^{2+}, Ni^{2+}, Zn^{2+}, and Co^{2+}, respectively, as shown in Table 3.

3.3.3. Temkin model

The Temkin isotherm model [38] contains a factor that explicitly takes an account of biosorbent–adsorbate interactions. By ignoring the extremely low and high values of concentrations, the model assumes that the heat of biosorption (function of temperature) of all molecules in the layer would decrease linearly rather than logarithmically with coverage as implied in the Freundlich equation [37]. The Temkin Eq. (8) is expressed as:

$$q_e = \frac{RT}{b}\ln K_T + \frac{RT}{b}\ln C_e \tag{8}$$

where $RT/b = B$ (J/mol), which is Temkin constant related to the heat of sorption, K_T is the equilibrium binding constant corresponding to the maximum binding energy (L/mg), R is the universal gas constant (8.314 J/mol K), and T is the absolute temperature (K). Further, Eq. (8) deduced to a linear form:

$$q_e = B\ln K_T + B\ln C_e \tag{8(a)}$$

From Eq. (8(a)), its derivation is characterized by a uniform distribution of binding energies, whereas B and K_T can be calculated from the slope (B) and intercepts (B ln K_T) by plotting the quantity sorbed q_e against ln C_e. The best fit of the experimental data and correlation coefficients were higher than 0.9 (Table 3) indicating the applicability of the Temkin isotherm model. The maximum binding energy was found to be 0.176, 0.458, 0.059, 0.106, and 0.295 J/mol for Zn^{2+}, Cu^{2+}, Mn^{2+}, Co^{2+}, and Ni^{2+}, respectively, as shown in Table 3.

3.3.4. Dubinin–Radushkevich model

The D–R model is an isotherm model [39], which does not assume a homogeneous surface or constant adsorption potential. It is generally applied to express the adsorption mechanism with a Gaussian energy distribution onto a heterogeneous surface.

The D–R Eq. (9) is given by

$$qe = qm\ exp\left(-K_\epsilon^2\right) \tag{9}$$

Its linear form of Eq. (10) can be given as

$$\ln q_e = \ln q_m - K_\varepsilon^2 \tag{10}$$

where q_e (mg/g) is the amount of the adsorbate adsorbed at equilibrium, q_m (mg/g) is the theoretical saturation capacity, K is a D–R constant related to the mean free energy of adsorption, and ε is the Polanyi potential; it can be calculated in the following equation:

$$RT\ln(1 + (1/C_e)) \tag{11}$$

where R (8.314 J/mol k) is the gas constant, and T (K) is the temperature. The values of q_m and K were determined by plotting ln q_e vs ε^2. The mean biosorption energy (E_s) (kJ/mol) can be calculated using the following equation:

$$E_s = 1/\sqrt{2K} \tag{12}$$

If the values of $E_s < 8$ KJ/mol, the biosorption process is physisorption, while for values of E_s is between 8 and 16 kJ/mol, the process is of chemisorptions or by ion-exchange. Based on the experimental results, the mean energy value (E_s = 5 to 7 kJ/mol) of biosorption for heavy metals shows the interaction between adsorbent and adsorbate by physical adsorption [39] which is shown in Table 3.

3.3.5. Error analysis

Error function has been used to find out the most suitable isotherm model to represent the experimental data. The average relative error (ARE %) function was employed to minimize the fractional error and test criterion for the fit of the correlations. It measures the differences of the amount of heavy metals adsorbed onto the biosorbent (q_e), measured experimentally and the predicted values using the following equation:

$$\mathrm{ARE}\,(\%) = 100/\mathrm{n}\sum_{\mathrm{i}=0}^{\mathrm{n}}\left(\mathrm{q_e exp} - \mathrm{q_e cal}/\mathrm{q_e exp}\right) \tag{13}$$

where $q_e$cal is each value of q_e predicted by the fitted model, $q_e$exp is each value of q_e measured experimentally, and n is the number of experiments performed. The percent of ARE values for Langmuir, Freundlich, Temkin, and D–R are illustrated in Table 3. Based on the data of ARE (%) and correlation coefficients (R^2), Freundlich isotherm model gives the best fit and D–R was found to be least fit in the biosorption equilibrium data.

3.4. Fixed bed column studies

3.4.1. Effect of bed height (Biosorbent mass)

The effect of varying the bed-loading extent during the experiments has a significant effect on column performance due to the number of active sites available for biosorption of metal ions. Experimental parameters for the effect of bed height were carried out at 5, 10, 15, 20, and 25 cm with varying the flow rate of 1–10 mL/min, at actual pH. The breakthrough curve obtained for biosorption of Zn^{2+}, Cu^{2+}, Mn^{2+}, Co^{2+}, and Ni^{2+} onto EMB by increasing the bed packed length from 5, 15, and 25 cm at constant influent flow rate of 1 mL/min was shown in Fig. 7(a)–(c). From Fig. 7(a), earlier breakthrough was attained due to the lower bed height and there is a sharp rise after the breakthrough point due to the exit of MTZ. The rapid passage of influent through the small bed column leads to limitation in heavy metal biosorption by EMB. In addition, from the Fig. 7(b) and (c), it was found that longer time was taken for the breakthrough point. From the plots, it is shown that the breakthrough time, t_b, and saturation time, t_s, were found to increase with an increase in the bed height. The plots represent that the shape and gradient of the breakthrough curves were slightly different with the variation of bed depth. An increase in metal ions uptake was observed at elevated bed height due to the increase in the amount of the EMB. This provides more fixations of the cations with the active binding sites for the biosorption process, and the increase of biosorbent mass provides a larger surface area leading to an increase in the volume of the treated solution. As the bed height increases, simultaneously, the MTZ also gets increased in the column which moves downwards from the entrance of the bed to the exit [2]. Hence for same influent concentration and fixed bed system, an increase in bed height would create a longer distance for the MTZ to reach the exit subsequently resulting in an extended breakthrough time [40].

3.4.2. Effect of flow rate

The effect of influent flow rate is an important parameter as it determines the contact time of the effluent with the biosorbent in the fixed bed column. The breakthrough curves C_t/C_o against time (min) for three different flow rates (1, 5, and 10 mL/min) at a constant fixed bed height of 25 cm are illustrated in Fig. 8(a)–(c), respectively. From the figure, as the flow rate increased, the breakthrough curve becomes steeper and it was found that biosorbent gets saturated early at 10 mL/min. The main reason for this behavior

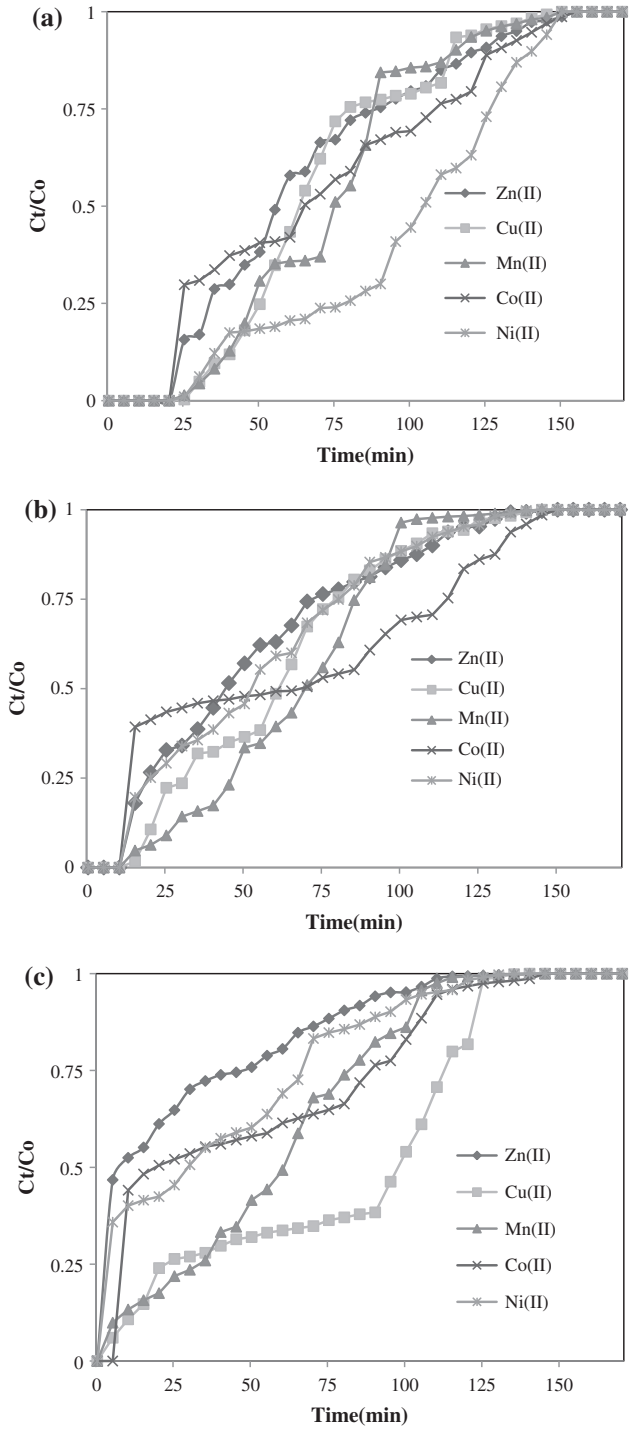

Fig. 8. ((a), (b), and (c)) Effect of influent flow rate on biosorption of heavy metal ions in fixed bed column. [Conditions: influent flow rate: 1, 5, and 10 mL/min; constant bed height of 25 cm; temperature: 303 K.]

is due to the increase in the movement of the MTZ, which results time required to reach the desired breakthrough concentration decreases [28]. From Fig. 8(a),

Table 4
Thomas model parameters for the removal of heavy metals (Zn, Cu, Mn, Co, and Ni) from electroplating effluent by EMB at different conditions using linear regression analysis

Bed height	Flow rate	Zn(II)			Cu(II)			Mn(II)			Co(II)			Ni(II)		
Z (cm)	Q_F (mL/min)	k_{th} (mL/min mg)	q_o (mg/g)	R^2	k_{th} (mL/min mg)	q_o (mg/g)	R^2	k_{th} (mL/min mg)	q_o (mg/g)	R^2	k_{th} (mL/min mg)	q_o (mg/g)	R^2	k_{th} (mL/min mg)	q_o (mg/g)	R^2
5	1	0.0017	54.94	0.94	0.009	9.874	0.93	0.0004	425	0.92	0.0059	22.98	0.95	0.0059	15.25	0.93
15	1	0.0018	76	0.92	0.0099	15.35	0.92	0.0006	457.77	0.97	0.0048	28.98	0.93	0.0061	22.21	0.79
25	1	0.0016	105.58	0.97	0.011	28.19	0.91	0.0005	599.33	0.96	0.0037	39.47	0.9	0.0061	44.36	0.89
25	5	0.0093	78.49	0.93	0.0507	21.32	0.95	0.003	485.77	0.97	0.0143	32.47	0.77	0.035	23	0.93
25	10	0.019	30.52	0.93	0.0807	24.37	0.67	0.0054	405.43	0.92	0.037	18.88	0.85	0.0671	14.89	0.89

the breakthrough capacity ($Q_{0.5}$), takes place at 55.5 min (Zn^{2+}), 63.1 min (Cu^{2+}), 74.5 min (Mn^{2+}), 64.9 min (Co^{2+}), and 104.5 min (Ni^{2+}) BV with influent flow rate of 1 mL/min. Similarly from the Fig. 8(b) and (c), the breakthrough capacity ($Q_{0.5}$), occurs at 44.8 min (Zn^{2+}), 61.5 min (Cu^{2+}), 69.5 min (Mn^{2+}), 70 min (Co^{2+}), and 52.5 min (Ni^{2+}), and 7.6 min (Zn^{2+}), 97.5 min (Cu^{2+}), 60.5 min (Mn^{2+}), 19.8 min (Co^{2+}), and 29.8 min (Ni^{2+}) with influent flow rates of 5 and 10 mL/min, respectively. In addition, the EBRT was found to be 4.461, 2.547, and 1.433 min for flow rates 1, 5, and 10 mL/min. This experimental data indicate that higher EBRT has more time to contact, which resulted in higher removal of metal ions in the column [40,41].

3.5. Modeling of breakthrough curves

Fixed bed column data obtained were further optimized for their breakthrough behaviors using two different mathematical equation models like Thomas [42] and Yoon–Nelson [43] to explore the biosorption mechanism. Execution of Thomas model was necessary to be carried out in order to predict the breakthrough curve, maximum metal sorption capacity of the column (q_o), and the Thomas rate constant (k_{Th}). Similarly, Yoon–Nelson model allows to find out the time required for 50% breakthrough, (τ), and the Yoon–Nelson rate constant, (k_{YN}).

3.5.1. Applications of the Thomas model

Thomas model is based on the assumption that the process follows Langmuir isotherms of equilibrium with no axial dispersion and plug flow behavior in the bed. In addition, this model assumes that the rate driving force obeys the second-order reversible reaction kinetics [40,42]. The linearized form of Thomas model can be expressed as follows (Eq. (14)),

$$\ln\left(\frac{C_o}{C_t}-1\right)=\frac{k_{Th}\ q_o\ m}{v}-\frac{k_{Th}\ C_o}{vt} \tag{14}$$

where k_{Th} (mL/mg/min) is the Thomas rate constant, q_o (mg/g) is the equilibrium adsorbate uptake per gram of the biosorbent, C_o and C_t (mg/L) are the inlet and outlet concentrations (g), m is the mass of biosorbent in the column, and v (mL/min) stands for flow rate. The value C_t/C_o is the ratio of outlet to inlet heavy metal concentrations. By plotting the linear plots of ln [(C_o/C_t)–1] against time (t), the rate constant value (k_{Th}) was determined and the maximum capacity of sorption (q_o) was obtained from the slope and intercepts using values from the column

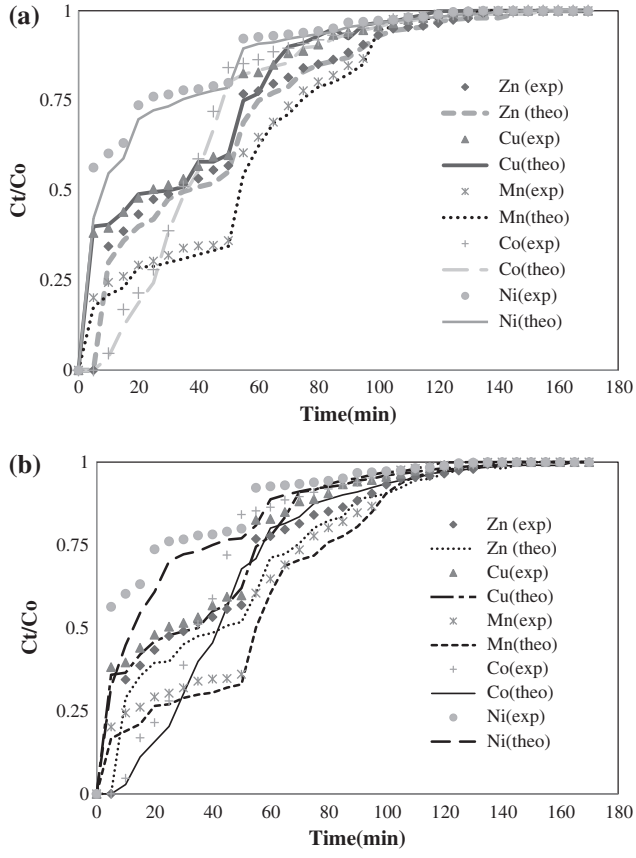

Fig. 9. ((a) and (b)) Comparison of the experimental and predicted breakthrough curves according to the Thomson model and Yoon–Nelson model. [Conditions: Bed height: 5 cm; influent flow rate: 1 mL/min; temperature: 303 K.]

experiments. From Table 4, it was observed that by increasing the flow rate, the maximum biosorption capacity (q_o) decreased but the values of rate constant (k_{Th}) increased. Further, it is seen by extending the bed height, the values of q_o are decreased and k_{Th} value increased significantly for all the five heavy metals. In addition, from Table 4, it was found that at 25 cm of bed height with 1 mL/min flow rate gives maximum biosorption values (q_o) of 599.33, 105.58, 44.36, 39.47, and 28.19 mg/g for Mn^{2+}, Zn^{2+}, Ni^{2+}, Co^{2+}, and Cu^{2+}, respectively. Based on observation, higher bed height with lower flow rate would increase the uptake of heavy metals on the fixed bed column. Further, the comparison of the experimental (points) and predicted breakthrough curves (lines) are shown in Fig. 9(a). It is clear from Fig. 9(a), the experimental values were very close to the predicted values according to the Thomson model. From the correlation coefficients (R^2), predicated and experimental values, and other parameters Table 4, it can be concluded that the experimental data fitted well with Thomson model.

Table 5
Yoon–Nelson model parameters for the removal of heavy metals (Zn, Cu, Mn, Co, and Ni) from electroplating effluent by EMB at different conditions using linear regression analysis

Bed height	Flow rate	Zn(II)			Cu (II)			Mn(II)			Co(II)			Ni(II)		
Z (cm)	Q_F (mL/min)	K_{YN}	τ (min)	R^2	K_{YN}	T (min)	R^2	K_{YN}	τ (min)	R^2	K_{YN}	τ (min)	R^2	K_{YN}	τ (min)	R^2
5	1	0.042	33.35	0.94	0.048	27.77	0.93	0.056	45.53	0.92	0.054	37.66	0.95	0.04	3.1	0.93
15	1	0.045	55.6	0.92	0.053	43.01	0.92	0.07	58.85	0.97	0.044	47.43	0.93	0.041	49.58	0.79
25	1	0.041	61.8	0.97	0.063	73.84	0.91	0.06	74.91	0.96	0.034	64.44	0.9	0.041	99	0.89
25	5	0.045	48.66	0.93	0.054	60.07	0.95	0.07	62.45	0.97	0.026	53.57	0.77	0.047	51.4	0.93
25	10	0.046	18.91	0.93	0.043	68.02	0.67	0.063	52.12	0.92	0.034	35.85	0.85	0.045	33.31	0.89

3.5.2. Application of Yoon–Nelson model

A theoretical model was developed by Yoon–Nelson, based on the assumption that the rate of decrease in the probability of biosorption for each adsorbate molecule is proportional to the probability of adsorbate biosorption and the probability of adsorbate breakthrough on the biosorbent [44,45]. The linearized model for a single component system is expressed as Eq. (15):

$$\ln\left(\frac{C_t}{C_o - C_t}\right) = k_{YN}\ t - \tau k_{YN} \tag{15}$$

where k_{YN} (min^{-1}) is the Yoon–Nelson rate constant, and τ (min) is the time required for 50% adsorbate breakthrough. The values of k_{YN} and τ were estimated from slope and intercepts of the linear graph between ln $[(C_t)/(C_o - C_t)]$ vs. time t at different flow rates, bed heights, and initial concentrations, and the data are illustrated in Table 5. From Table 5, it was observed that the values of k_{YN} increase with an increase in flow rates, while the corresponding values of τ (the time required for 50% breakthrough) are noticed to decrease. Nevertheless, the values of k_{YN} decrease with an increase in bed height, whereas, a reverse trend was observed in the value of τ . In addition, it was found that τ (min) values of 99 min (Ni^{2+}), 74.91 min (Mn^{2+}), 73.84 min (Cu^{2+}), 64.44 min (Co^{2+}), and 61.80 min (Zn^{2+}) were obtained at 25 cm of bed height and 1 mL/min flow rate. In addition, the experimental breakthrough curves (points) were good correlation to the theoretical breakthrough curves (lines) according to Yoon–Nelson model as shown in Fig. 9(b). In comparison of values R^2 (Table 5) for all the breakthrough curves, and experimental and theoretical data, the model proposed by Yoon–Nelson model could be well fitted with the experimental results.

4. Conclusion

In this paper, the biosorption behaviour of heavy metals onto encapsulated EMB was investigated by performing batch and fixed bed column studies. From the batch experiments, Cu^{2+} shows maximum efficiency of about 99.3%, followed by Ni^{2+} (77.98%), Co^{2+} (70.80%), Zn^{2+} (60.90%), and Mn^{2+} (49.96%) and the equilibrium data well fitted with Langmuir, Freundlich, and Temkin models. The column was found to perform better with lower flow rate (1 mL/min) and with higher bed height (25 cm). The maximum removal efficiency of heavy metals was found to be Cu^{2+} (99.69%), Ni^{2+} (98.92%), Mn^{2+} (98.59), Zn^{2+} (84.21%), and Co^{2+} (70.57%) and the data fitted well with both Thomson and Yoon–Nelson models. Overall, EMB proved to be an eco-friendly and potential biosorbent for the removal of heavy metals from electroplating wastewater and it can be considered for the pilot-scale studies.

Acknowledgment

The authors would like to thank Nanotechnology Research Centre, SRM University, Chennai, for helping them with instrumentation facilities for this work.

References

[1] D.H.K. Reddy, D.K.V. Ramana, K. Seshaiah, A.V.R. Reddy, Biosorption of Ni(II) from aqueous phase by *Moringa oleifera* bark, a low cost biosorbent, Desalination 268 (2011) 150–157.
[2] J. Goel, K. Kadirvelu, C. Rajagopal, V. Kumar Garg, Removal of lead(II) by adsorption using treated granular activated carbon: Batch and column studies, J. Hazard. Mater. 125 (2005) 211–220.
[3] G.E. Cartwright, M.M. Wintrobe, Copper metabolism in normal subjects, Am. J. Clin. Nutr. 14 (1964) 224–232.

[4] J. Bland, A story of trace mineral induced behavioural disorders and hair mineral analysis, Am. J. Orthopsych. 9 (1980) 24–32.
[5] D.R. Bennett, Zinc toxicity following massive coin ingestion, Am. J. Forensic Med. Pathol. 18 (1997) 148–153.
[6] L. Cai, X.K. Li, Y. Song, M.G. Cherian, Essentiality, toxicology and chelation therapy of zinc and copper, Curr. Med. Chem. 12 (2005) 2753–2763.
[7] J. Crossgrove, W. Zheng, Manganese toxicity upon overexposure, NMR Biomed. 17 (2004) 544–553.
[8] G. McMillan, Is electric arc welding linked to manganism or Parkinson's disease? Toxicol. Rev. 24 (2005) 237–257.
[9] L.R. Goldfrank, Goldfrank's Toxicologic Emergencies, ninth ed., McGraw-Hill Medical, New York, NY, 2011.
[10] Z. Shi, Nickel carbonyl: Toxicity and human health, Sci. Total Environ. 148 (1994) 293–298.
[11] E. Denkhaus, K. Salnikow, Nickel essentiality, toxicity, and carcinogenicity, Crit. Rev. Oncol. Haematol. 42 (2002) 35–56.
[12] B. Ramavandi, S. Farjadfard, Removal of chemical oxygen demand from textile wastewater using a natural coagulant, Korean. J. Chem. Eng. 31 (2014) 81–87.
[13] G. Asgari, B. Ramavandi, L. Rasuli, M. Ahmadi, Cr (VI) adsorption from aqueous solution using a surfactant-modified Iranian zeolite: Characterization, optimization, and kinetic approach, Desalin. Water Treat. 51 (2013) 6009–6020.
[14] N. Beyazit, Batch and column studies on zinc removal from industrial wastewater using natural clinoptilolite: Factors affecting sorption capacities and kinetics, Toxicol. Environ. Chem. 95 (2012) 45–68.
[15] A.G. Paulino, A.J. Cunha, R.V.S. Alfaya, A.A.S. Alfaya, Chemically modified natural cotton fiber: A low-cost biosorbent for the removal of the Cu (II), Zn (II), Cd (II), and Pb(II) from natural water, Desalin. Water Treat. 52 (2014) 4223–4233.
[16] H. Daraei, A. Mittal, J. Mittal, H. Kamali, Optimization of Cr(VI) removal onto biosorbent eggshell membrane: Experimental and theoretical approaches, Desalin. Water Treat. 52 (2013) 1307–1315.
[17] T.S. Anirudhan, P.G. Radhakrishnan, Experimental studies and design of batch reactor for sorption of Cu (II) ions onto polymerized tamarind fruit shell cation exchanger, Chem. Eng. Commun. 200 (2013) 798–819.
[18] A.H. Sulaymon, D.W. Abbood, A.H. Ali, Removal of phenol and lead from synthetic wastewater by adsorption onto granular activated carbon in fixed bed adsorbers: Prediction of breakthrough curves, Desalin. Water Treat. 40 (2012) 244–253.
[19] S.M. Lee, W.G. Kim, J.K. Yang, D. Tiwari, Sorption behaviour of manganese-coated calcined-starfish and manganese-coated sand for Mn(II), Environ. Technol. 31 (2010) 445–453.
[20] A.F. Shaaban, D.A. Fadel, A.A. Mahmoud, M.A. Elkomy, S.M. Elbahy, Removal of Pb(II), Cd(II), Mn (II), and Zn(II) using iminodiacetate chelating resin by batch and fixed-bed column methods, Desalin. Water Treat. 51 (2013) 5526–5536.
[21] Y. Li, B. Zhao, L. Zhang, R. Han, Biosorption of copper ion by natural and modified wheat straw in fixed-bed column, Desalin. Water Treat. 51 (2013) 5735–5745.
[22] M.A. Acheampong, J.P.C. Pereira, R.J.W. Meulepas, P.N.L. Lens, Kinetics modelling of Cu(II) biosorption on to coconut shell and *Moringa oleifera* seeds from tropical regions, Environ. Technol. 33 (2012) 409–417.
[23] H.N. Bhatti, B. Mumtaz, M.A. Hanif, R. Nadeem, Removal of Zn(II) ions from aqueous solution using *Moringa oleifera* Lam. (horseradish tree) biomass, Process Biochem. 42 (2007) 547–553.
[24] D.H.K. Reddy, K. Seshaiah, A.V.R. Reddy, M. Rao, M.C. Wang, Biosorption of Pb^{2+} from aqueous solutions by *Moringa oleifera* bark: Equilibrium and kinetic studies, J. Hazard. Mater. 174 (2010) 831–838.
[25] K. Bandhyopadhyay, D. Das, P. Bhattacharyya, B.R. Maiti, Reaction engineering studies on biodegradation of phenol by *Pseudomonas putida* MTCC 1194 immobilized on calcium alginate, Biochem. Eng. J. 8 (2001) 179–186.
[26] A. Domínguez, S.R. Couto, A. Sanromán, Dye decolorization by *Trametes hirsuta* immobilized into alginate beads, J. Microbiol. Biotechnol. 21 (2005) 405–409.
[27] E. Malkoc, Y. Nuhoglu, Y. Abali, Cr(VI) adsorption by waste acorn of *Quercus ithaburensis* in fixed beds: Prediction of breakthrough curves, Chem. Eng. J. 119 (2006) 61–68.
[28] M. Bhaumik, K. Setshedi, A. Maity, M.S. Onyango, Chromium(VI) removal from water using fixed bed column of polypyrrole/Fe_3O_4 nanocomposite, Sep. Purif. Technol. 110 (2013) 11–19.
[29] A. Farooq, U. Rashid, Physico-chemical characteristic of *Moringa oleifera* seeds and seed oil from a wild provenance of Pakistan, Pak. J. Bot. 39 (2007) 1443–1453.
[30] C.S.T. Araújo, E.I. Melo, V.N. Alves, N.M.M. Coelho, *Moringa oleifera* Lam. seeds as a natural solid adsorbent for removal of AgI in aqueous solutions, J. Braz. Chem. Soc. 21 (2010) 1727–1732.
[31] S.M. de Oliveira Brito, H.M.C. Andrade, L.F. Soares, R.P. de Azevedo, Brazil nut shells as a new biosorbent to remove methylene blue and indigo carmine from aqueous solutions, J. Hazard. Mater. 174 (2010) 84–92.
[32] K. Ravikumar, A.K. Sheeja, Heavy metal removal from water using *Moringa oleifera* seed coagulant and double filtration, Int. J. Scie. Eng. Res. 4 (2013) 10–13.
[33] D. Fang, R. Zhang, W. Deng, J. Li, Highly efficient removal of Cu(II), Zn(II), Ni(II) and Fe(II) from electroplating wastewater using sulphide from sulphidogenic bioreactor effluent, Environ. Technol. 33 (2012) 1709–1715.
[34] S.R. Taffarel, J. Rubio, Removal of Mn^{2+} from aqueous solution by manganese oxide coated zeolite, Miner. Eng. 23 (2010) 1131–1138.
[35] Y.H. Li, T.L. Du, J. Sun, Y. Xia, Z. Wang, W. Zhang, K. Wang, H. Zhu, D. Wu, Adsorption of cationic red X-GRL from aqueous solutions by graphene: Equilibrium, kinetics and thermodynamics study, Chem. Biochem. Eng. 25 (2011) 483–491.
[36] I. Langmuir, The constitution and fundamental properties of solids and liquids. Part I. Solids, J. Am. Chem. Soc. 38 (1916) 2221–2295.
[37] H.M.F. Freundlich, Over the adsorption in solution, Z. Phys. Chem. 57A (1906) 385–470.
[38] M.J. Temkin, V. Pyzhev, Kinetics of ammonia synthesis on promoted iron catalyst, Acta Phys. Chim. USSR 12 (1940) 327–356.

[39] S. Tunali, T. Akar, A.S. Özcan, I. Kiran, A. Özcan, Equilibrium and kinetics of biosorption of lead(II) from aqueous solutions by *Cephalosporium aphidicola*, Sep. Purif. Technol. 47 (2006) 105–112.
[40] Z.Z. Chowdhury, S.M. Zain, A.K. Rashid, R.F. Rafique, K. Khalid, Breakthrough curve analysis for column dynamics sorption of Mn(II) ions from wastewater by using *Mangostana garcinia* peel-based granular-activated carbon, J. Chem. 2013 (2013) 1–8.
[41] X. Lin, R. Li, Q. Wen, J. Wu, J. Fan, X. Jin, W. Qian, D. Liu, X. Chen, Y. Chen, J. Xie, J. Bai, H. Ying, Experimental and modeling studies on the sorption breakthrough behaviors of butanol from aqueous solution in a fixed-bed of KA-I resin, Biotechnol. Bioprocess Eng. 18 (2013) 223–233.
[42] H.C. Thomas, Chromatography: A problem in kinetics, Ann. N.Y. Acad. Sci. 49 (1948) 161–182.
[43] Y.H. Yoon, J.H. Nelson, Application of gas adsorption kinetics I. A theoretical model for respirator cartridge service life, Am. Ind. Hyg. Assoc. J. 45 (1984) 509–516.
[44] A.A. Ahmad, B.H. Hameed, Fixed-bed adsorption of reactive azo dye onto granular activated carbon prepared from waste, J. Hazard. Mater. 175 (2010) 298–303.
[45] Y. Long, D. Lei, J. Ni, Z. Ren, C. Chen, H. Xu, Packed bed column studies on lead(II) removal from industrial wastewater by modified *Agaricus bisporus*, Bioresour. Technol. 152 (2014) 457–463.